GaAs/AlGaAs self-sensing cantilevers for low temperature scanning probe microscopy

R. G. Beck, M. A. Eriksson, M. A. Topinka, and R. M. Westervelt[a)]
Department of Physics and Division of Applied Sciences, Harvard University, Cambridge, Massachusetts 02138

K. D. Maranowski and A. C. Gossard
Materials Department, University of California, Santa Barbara, California 93106

(Received 9 December 1997; accepted for publication 23 June 1998)

We have fabricated scanning probe microscope cantilevers with dimensions $65\times 11.4\times 0.25\ \mu m^3$ and $3\times 2\times 0.129\ \mu m^3$ from GaAs/$Al_{0.3}Ga_{0.7}As$ heterostructures containing two-dimensional electron gases. Deflection is measured by an integrated field-effect transistor (FET) that senses strain via the piezoelectric effect and provides a low noise, low power displacement readout. We present images of a 200 nm mica grating taken with the large cantilever having a deflection (force) noise 10 Å/$\sqrt{\text{Hz}}$ (19 pN/$\sqrt{\text{Hz}}$) at $T=2.2$ K. The small cantilever has a resonant frequency of 11 MHz, a FET gate charge noise of 0.001 $e/\sqrt{\text{Hz}}$, and is projected to have a deflection (force) noise of 0.002 Å/$\sqrt{\text{Hz}}$ (1 pN/$\sqrt{\text{Hz}}$) at $T=4.2$ K. © *1998 American Institute of Physics.* [S0003-6951(98)00734-7]

The invention of the atomic force microscope[1] has profoundly impacted surface imaging and has spurred the exploration of new types of scanning probe microscopy (SPM). The deflection of scanning probe cantilevers has been detected by using tunneling current,[1] optical levers and interferometers,[2] capacitance,[3] piezoresistance,[4] and piezoelectrics.[5–7] Recently, strain sensors have been demonstrated comprised of field-effect transistors (FETs) fabricated from a GaAs/AlGaAs heterostructure containing a two-dimensional electron gas (2DEG).[8,9] Such strain sensors can be used in heterostructure SPM cantilevers and also have broader potential applications for detecting forces and displacements in GaAs/AlGaAs microelectromechanical systems (MEMS).[10,11]

In this letter we describe the fabrication and operation of GaAs/$Al_{0.3}Ga_{0.7}As$ SPM cantilevers with integrated strain-sensing FETs. Strain-sensing FETs offer advantages for cantilever deflection sensing. Because the strain sensor is integrated into the cantilever, no external deflection sensors are needed, and micron-scale cantilevers and more complex microelectromechanical systems become feasible. Both force and displacement sensitivity of strain-sensing cantilevers improve with scaling to smaller sizes, and the resonant frequency increases. The strain-sensing FET provides gain, reducing the cantilever power dissipation by several orders of magnitude compared with piezoresistive strain sensors. Small size, high operating frequency, and low power dissipation make strain-sensing FETs ideal for use in small cantilevers[12] and other MEMS.

The large (small) cantilevers described here have dimensions $65\times 11.4\times 0.25\ \mu m^3$ $(3\times 2\times 0.129\ \mu m^3)$. We have characterized integrated FETs in both cantilevers in the first demonstration of functional electronic devices integrated into thin free-standing structures containing 2DEGs. The large cantilever is used to demonstrate scanning probe capabilities while the small cantilever represents an advance in fabrication and points toward advantages of smaller cantilevers. The FET noise for both cantilevers has a $1/f$ spectrum between 10 Hz and 2 kHz with $\delta V_g = 1(0.06)\ \mu\text{V}/\sqrt{\text{Hz}}$ at 100 Hz corresponding to a gate charge noise $\delta Q_g \sim 0.1(0.005) e/\sqrt{\text{Hz}}$ where δV_g and δQ_g are the gate voltage and charge noise. The cantilevers have calculated spring constants of 0.019 (4.7) N/m and resonant frequencies of 46 kHz (11 MHz). Vertical resolution was measured (projected) to be 10 (0.018) Å/$\sqrt{\text{Hz}}$ at 100 Hz corresponding to a force resolution of 19(3) pN/$\sqrt{\text{Hz}}$, limited by FET noise. We imaged a mica grating with the large cantilever at $T=2.2$ K.

Figures 1(a) and 1(b) show scanning electron microscopy (SEM) images of the large and small cantilevers with

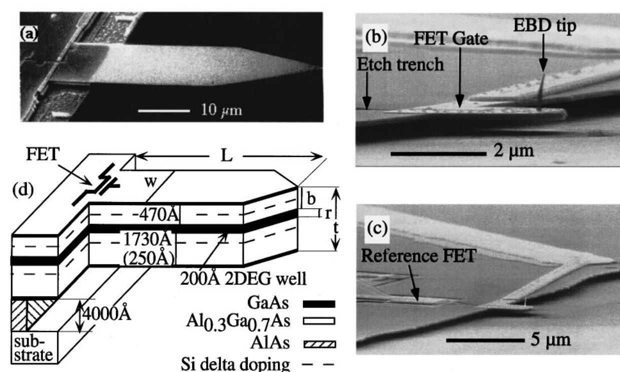

FIG. 1. (a) SEM image showing a GaAs/AlGaAs cantilever, $65\times 11.4 \times 0.25\ \mu m^3$, with a strain-sensing field-effect transistor (FET) at its base. Both the FET gate and an etch trench can be seen at the cantilever base showing that electrons flow through the region of maximum strain on the suspended structure of the cantilever. (b) SEM image of a smaller cantilever $3\times 2\times 0.129\ \mu m^3$ with an integrated strain-sensing FET and an electron beam deposited tip. The electrons are constrained to flow onto the suspended structure of the cantilever by the etch trench, which extends half the length of the cantilever. (c) View of the small cantilever plus reference FET, which enables a differential strain measurement. (d) Schematic diagram of the epitaxial layer structure of the wafer and cantilever. The dimension in parentheses applies only to the small cantilever.

[a)]Electronic mail: westervelt@fas.harvard.edu

Downloaded 26 Mar 2001 to 140.247.57.93. Redistribution subject to AIP copyright, see http://ojps.aip.org/aplo/aplcr.jsp

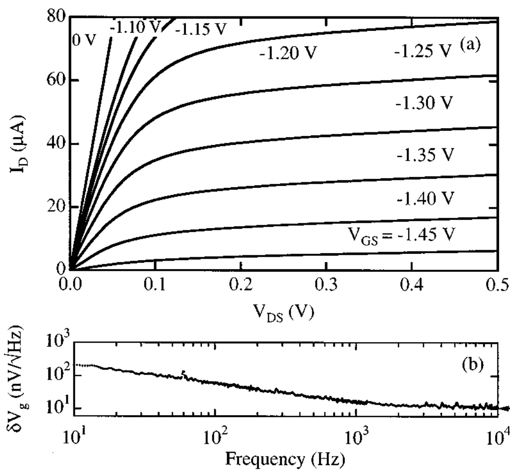

FIG. 2. (a) Drain characteristics for the FET on the large cantilever taken at $T=4.2$ K for the gate-source voltages indicated. (b) Measured voltage noise referred to the input of the FET on the small free-standing cantilever. At 2 kHz, FET noise is dominated by the noise from the external amplifier. The arrow indicates a voltage noise corresponding to a gate charge noise of $0.001e/\sqrt{\text{Hz}}$.

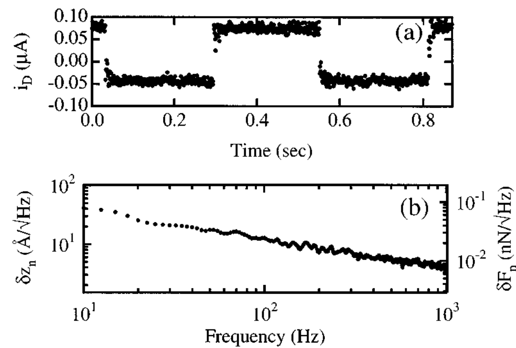

FIG. 3. (a) FET response as the large cantilever is deflected at a frequency of 2 Hz by a step deflection of amplitude 0.4 μm corresponding to a step force of 7.6 nN. (b) Measured noise spectra of the FET on the large free-standing cantilever converted to units of deflection and force noise.

integrated strain-sensing FETs. Figure 1(c) shows the small cantilever plus an additional on-chip reference FET. Figure 1(d) is a schematic diagram of the epitaxial layers in the heterostructure. The layers composing the cantilevers in growth order are 100 Å GaAs, 1510 Å (250 Å for the small lever) $Al_{0.3}Ga_{0.7}As$, Si delta doping layer, 220 Å $Al_{0.3}Ga_{0.7}As$, 200 Å GaAs, 220 Å $Al_{0.3}Ga_{0.7}As$, Si delta doping layer, 250 Å $Al_{0.3}Ga_{0.7}As$, and 50 Å GaAs. The cantilevers are oriented along the [011] direction for the maximum strain effect. The small cantilever is located ~40 μm from the edge of the chip.

Six electron beam lithography steps are required for small cantilever fabrication. For each step, resist is applied using an off-axis spinner chuck to eliminate the unwanted resist bead close to the fabrication region. First, AuNiGe contacts are deposited and thermally annealed. Second, the channels of the FETs are defined by etch trenches 650 Å deep made by ion milling. Third, the gate leads, gate contacts, and on-cantilever gate 8 μm long by 1 μm wide with a nominal gate-to-channel capacitance of $C_G=15$ fF were defined. A thin film of 50 Å Cr and 150 Å Au was thermally deposited. Fourth, the gate leads and contacts were made thicker by repatterning the gate layer, with the exception of the on-cantilever gate, and depositing 200 Å Cr and 1000 Å Au. Fifth, a vertical trench was cut around the cantilever using the ion miller to expose the underlying AlAs layer. After the resist is removed, the electron beam deposited (EBD) tip was grown on the cantilever by coating the sample with a thin layer of paraffin and placing the electron beam from the SEM on the end of the cantilever for 105 s with beam parameters of 15 keV and 3.0 pA. Residual paraffin was removed in Hexanes followed by an oxygen reactive ion etch. Finally, the cantilever was undercut and freed from the substrate by selectively etching the AlAs layer in a 1:15 solution of 49% HF:H_2O for 5 s. The fabrication of the large cantilever was similar.[13] The substrate beneath the large cantilever was cleaved away to facilitate contact with a sample for imaging.

Figure 2(a) shows drain characteristics I_D vs V_{DS} for the FET on the large cantilever at temperature $T=4.2$ K. For the large (small) lever, the small-signal transconductance is $g_m \cong 0.3(0.03)$ mS and drain source resistance is $r_{ds} \cong 50\ \text{k}\Omega$ (4 MΩ) at $I_D=50(10)$ μA. The pinchoff voltages are $V_{po} = V_{GS} = -1.5(-0.95)$ V. The cutoff frequency inferred from the transistor RC time is $g_m/2\pi C_G = 6(0.3)$ GHz. Figure 2(b) shows the gate voltage noise δV_g for the small on-cantilever FET. The noise power has a $1/f$ frequency dependence at least up to 2 kHz where it is dominated by the noise of the external amplifier. This white noise level corresponds to a low gate charge noise of $\delta q_n = C_G \delta V_g = 0.001e/\sqrt{\text{Hz}}$ which approaches the charge noise levels of single electron transistors.[14]

The large cantilever was mounted in vacuum as part of a low temperature scanning probe microscope.[15] Cantilever deflection was monitored by dc voltage biasing the FET channel and gate while monitoring the drain current with an Ithaco 1211 current amplifier. The bias point used for the measurements below was $V_{GS}=-1.30$ V and $V_{DS}=0.30$ V resulting in a power dissipation of 7.2 μW. Care was taken to shield the cantilever from the high voltages required to operate the SPM scanning tube. Images were taken at 4.2 and 2.2 K.

Figure 3(a) shows the current response of the large cantilever FET for a square wave deflection of the tip with a frequency of 2 Hz and peak-to-peak amplitude of 0.4 μm, corresponding to a tip force 7.6 nN. Figure 3(b) shows a graph of large cantilever deflection and force noise measured for a free-standing cantilever. The noise power has a $1/f$ spectrum in the frequency range between 10 Hz and 1 kHz and is independent of gate voltage and drain-source voltage in the operating region of the FET. The measured deflection sensitivity is limited by FET noise; mechanical thermal noise and amplifier noise are negligible.

Figure 4(a) presents a 7×7 μm^2 SPM image of a mica $\sin(x)\sin(y)$ calibration grating with period of 1 μm and a peak-to-peak amplitude of 200 nm taken using the large strain-sensing cantilever at $T=2.2$ K. Tip deflection was recorded in a 1 kHz bandwidth. Figure 4(b) with a smaller scan range demonstrates the finer vertical resolution of the cantilever.

Strain-sensing GaAs FETs operate via the piezoelectric effect. Deflection of the cantilever produces a polarization in the form of volume bound charge throughout the cantilever

Downloaded 26 Mar 2001 to 140.247.57.93. Redistribution subject to AIP copyright, see http://ojps.aip.org/aplo/aplcr.jsp

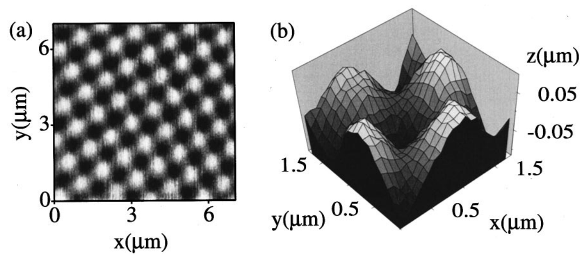

FIG. 4. (a) 7×7 μm^2 image taken using the large strain-sensing cantilever. The structure is a sin(x)sin(y) mica grating with spacing 1 μm and depth 200 nm. (b) A smaller scan demonstrating the finer resolution of the large cantilever.

and sheets of bound charge at every interface. In our model, we assume that free electrons in the FET channel screen the bound charge induced in the GaAs well and the two neighboring GaAs/AlGaAs interfaces producing an effective gate charge ΔQ. Assuming that the 2DEG is on the gate side of the cantilever [see Fig. 1(b)], the change in FET current ΔI for tip deflection Δz is

$$\Delta I = \frac{g_m \Delta Q(\Delta z)}{C_G} \cong \frac{3Eg_m brd_A}{\epsilon L^2}\,\Delta z, \tag{1}$$

where E is Young's modulus, d_A is the appropriate[16] piezoelectric constant d_{13} for $Al_{0.3}Ga_{0.7}As$, ϵ is the dielectric constant for $Al_{0.3}Ga_{0.7}As$, and the dimensions L, r, and b are indicated in Fig. 1(d). For the deflection shown in Fig. 3(a), Eq. (1) predicts $\Delta I = 0.14$ μA in good agreement[17] with the measured signal $\Delta I_m = 0.13$ μA. While most piezoelectric cantilevers are limited to dynamic operation faster than the dielectric relaxation time, strain-sensing FETs retain their function for static deflections, because the screening electrons provide the signal.

The advantages of strain-sensing FETs over other types of displacement sensors are manifested in how performance parameters scale to small sizes. Strain-sensing cantilevers gain sensitivity as their size is reduced. Consider a FET with a minimum detectable strain $\epsilon_{\min}$ at the cantilever surface. Both the minimum detectable force $F_{\min} = (Ewt^2/6L)\epsilon_{\min}$ and displacement $U_{\min} = (2L^2/3t)\epsilon_{\min}$ decrease as the cantilever is scaled to smaller sizes keeping the same aspect ratios. Assuming cantilever responsivity scales according to the screening model described by Eq. (1) and using the measured gate voltage noise for both FETs, the small cantilever has deflection sensitivity 0.002 Å/$\sqrt{\text{Hz}}$ and force sensitivity $\sim$1 pN/$\sqrt{\text{Hz}}$ greater than the large cantilever by factors of 4500 and 19, respectively. In addition, small cantilevers have high resonant frequencies and strain-sensing FETs have low power dissipation permitting operation in small structures. The power required for good sensitivity is typically $\sim$10 μW (see above). Commercial piezoresistive strain sensors[4] require much larger power $P_B \sim 1$ mW for good sensitivity, and the power required is independent of size scale for two-dimensional resistors. Comparing a piezoresistive cantilever[4] with our small self-sensing cantilever we find: (FET cantilever values in parentheses): spring constant 100 (4.7) N/m, resonant frequency 0.8 (11) MHz, deflection noise 0.002(0.002) Å/$\sqrt{\text{Hz}}$, force noise 20(1) pN/$\sqrt{\text{Hz}}$, and power dissipation $\sim$1 (0.005) mW. Thus, we achieve good sensitivity and high speed with low power dissipation. Small, fast strain-sensing FETs show promise for a range of sensitive high speed imaging applications.[12]

The authors would like to thank J. G. E. Harris, D. D. Awschalom, and J. Tien for help with cantilever fabrication. This work was supported at Harvard in part by ONR Award No. N00014-95-1-0104, the MRSEC program of the National Science Foundation under Award No. DMR-94-00396, and JSEP Award No. N00014-89-J-1023 and at UCSB under Award No. AFOSR F 49620-94-1-0158.

[1] G. Binnig, C. F. Quate, and C. Gerber, Phys. Rev. Lett. **56**, 930 (1986).
[2] D. Rugar, H. J. Mamin, R. Erlandsson, J. E. Stern, and B. D. Terris, Rev. Sci. Instrum. **59**, 2337 (1988).
[3] J. Brugger, N. Blanc, P. Renoud, and N. F. de Rooij, Sens. Actuators A **43**, 339 (1994).
[4] M. Tortonese, R. C. Barrett, and C. F. Quate, Appl. Phys. Lett. **62**, 834 (1992).
[5] S. Watanabe and T. Fujii, Rev. Sci. Instrum. **67**, 3898 (1996).
[6] T. Itoh and T. Suga, J. Vac. Sci. Technol. B **12**, 1581 (1994).
[7] J. Tansock and C. C. Williams, Ultramicroscopy **42–44**, 1464 (1992).
[8] R. G. Beck, M. A. Eriksson, R. M. Westervelt, K. L. Campman, and A. C. Gossard, Appl. Phys. Lett. **68**, 3763 (1996).
[9] A. K. Fung, L. Cong, J. D. Albrecht, M. I. Nathan, and P. P. Ruden, J. Appl. Phys. **81**, 502 (1997).
[10] A. N. Cleland and M. L. Roukes, Appl. Phys. Lett. **69**, 2653 (1996).
[11] T. S. Tighe, J. M. Worlock, and M. L. Roukes, Appl. Phys. Lett. **70**, 2687 (1997).
[12] D. A. Walters, J. P. Cleveland, N. H. Thomson, P. K. Hansma, M. A. Wendman, G. Gurley, and V. Elings, Rev. Sci. Instrum. **67**, 3583 (1996).
[13] R. G. Beck, M. A. Eriksson, R. M. Westervelt, K. D. Maranowski, and A. C. Gossard, Semicond. Sci. Technol. (to be published).
[14] D. V. Averin and K. K. Likharev, in *Single Charge Tunneling*, edited by H. Grabert and M. H. Devoret (Plenum, New York, 1991), pp. 311.
[15] M. A. Eriksson, R. G. Beck, M. Topinka, J. A. Katine, R. M. Westervelt, K. L. Campman, and A. C. Gossard, Appl. Phys. Lett. **69**, 671 (1996).
[16] K. Fricke, J. Appl. Phys. **70**, 914 (1991).
[17] This model assumes that channel electrons screen bound charge induced only in the 2DEG well and in the two neighboring GaAs/AlGaAs interfaces. Including the effect of the bound charge induced outside the well increases the calculated charge signal by a factor of 3.

Downloaded 26 Mar 2001 to 140.247.57.93. Redistribution subject to AIP copyright, see http://ojps.aip.org/aplo/aplcr.jsp